SPIE Optics+Photonics San Diego August 2011

Fabrication of complex structures with an array of nanopinhole cameras

Hartmut S. Leipner, Nadine Geyer*,
Frank Syrowatka, Huang Cheng, Bodo Fuhrmann

Interdisziplinäres Zentrum
für Materialwissenschaften
– Nanotechnikum Weinberg –

Martin-Luther-Universität Halle–Wittenberg

*Max-Planck-Institut für Mikrostrukturphysik Halle

Pinhole camera

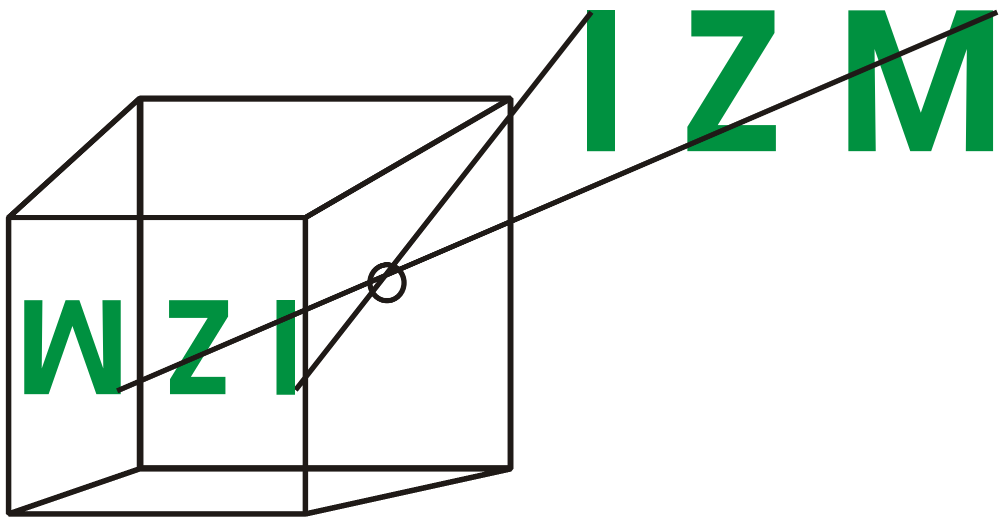

Scheme of a pinhole camera: Light from an object passes through a small hole to form an inverted image on the backside of a light-tight box.

Array of nanopinholes

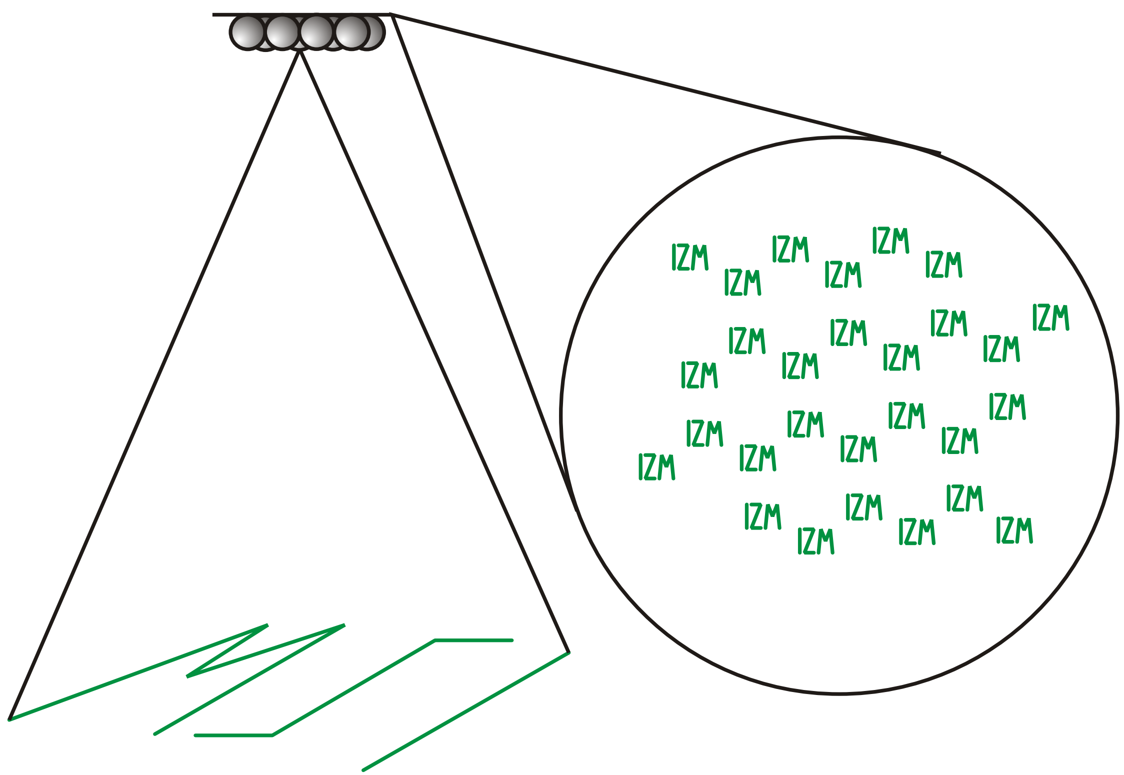

Nanopinhole cameras with particle beam instead of light.
A shaped thermal evaporation source may serve as an object.

Nanopinhole lithography

(a) (b) (c)

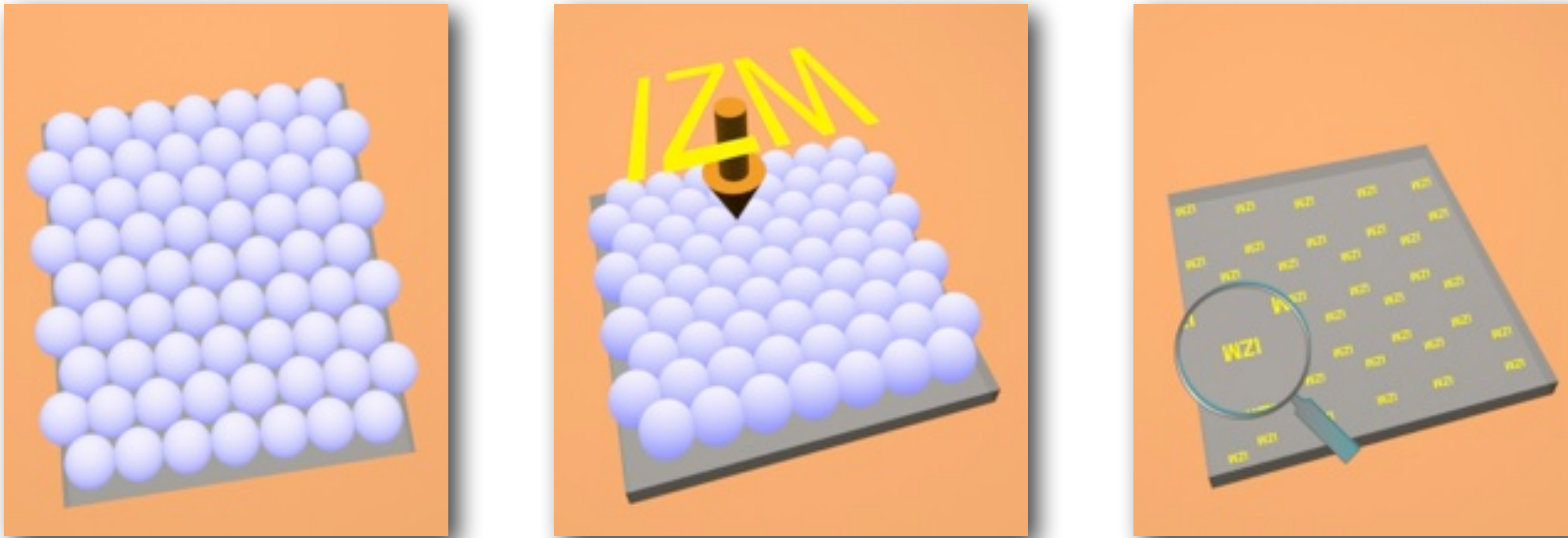

(*a*) Fabrication and modification of a mask consisting of polystyrene spheres

(*b*) Evaporation of a shaped metal source

(*c*) Removal of the mask; replicas of the source are remaining on the surface

Colloid lithography

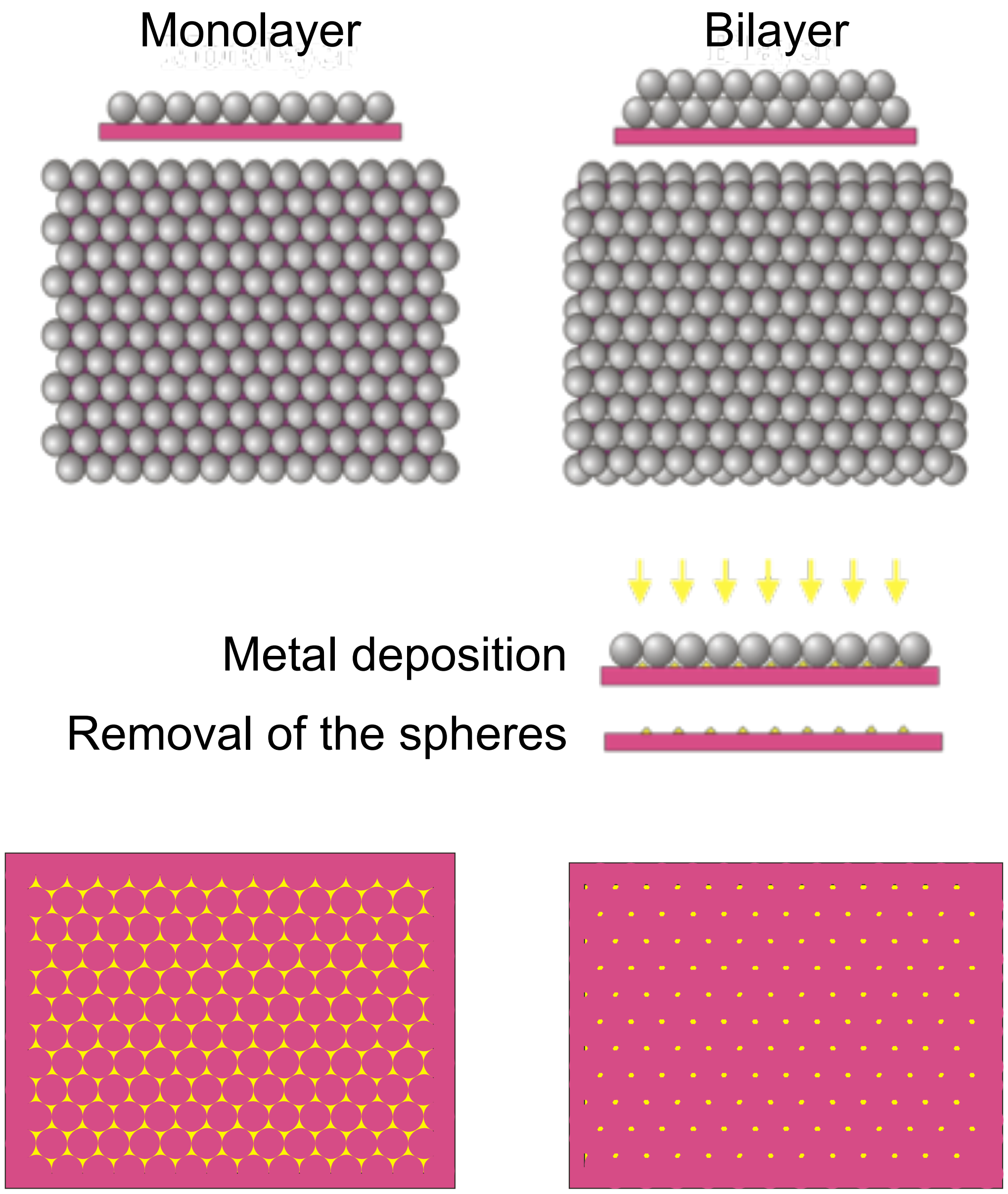

Hexagonal closed packed mono- or bilayers of monodisperse spherical particles serve as a lithographic mask.

Polystyrene (PS) particles with diameters in the range from 100 nm to 10 µm are used.

Arrangement of polystyrene spheres

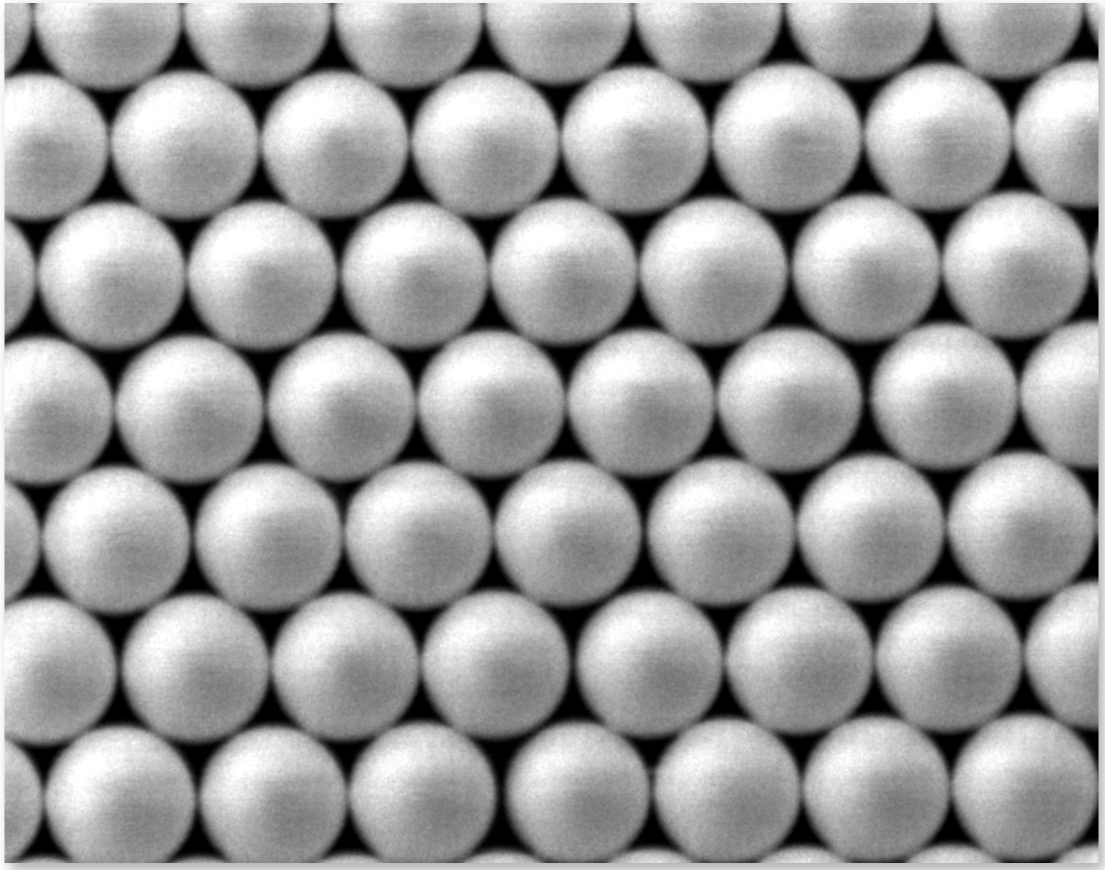

Field emission environmental scanning electron microscopy (ESEM) image of a layer of polystyrene spheres

Formation of 2D particle arrays

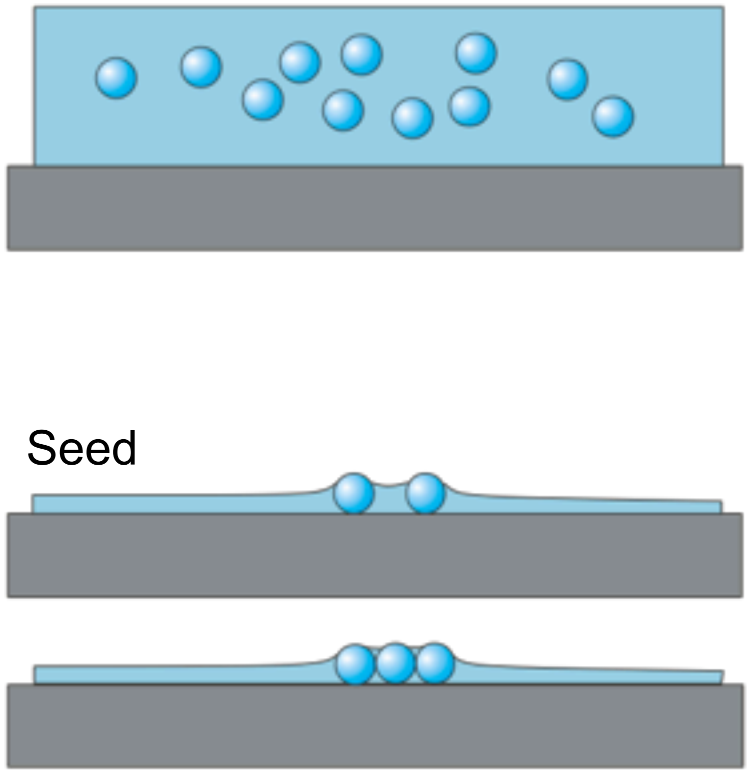

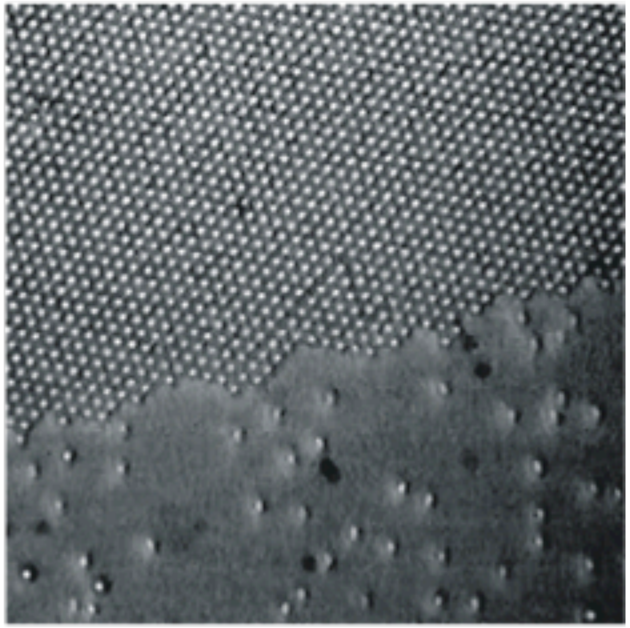

[Burmeister *et al*. Langmuir (1997)]

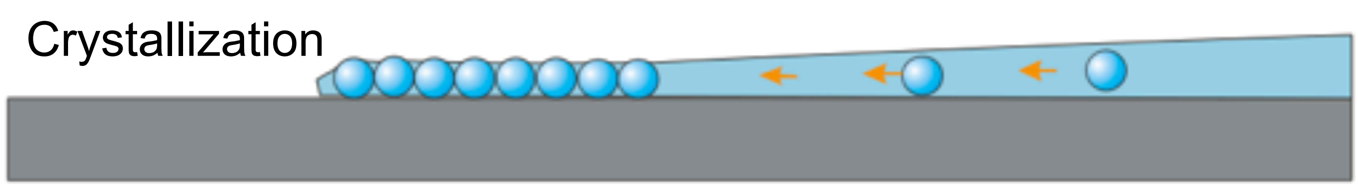

Formation of 2D particle arrays

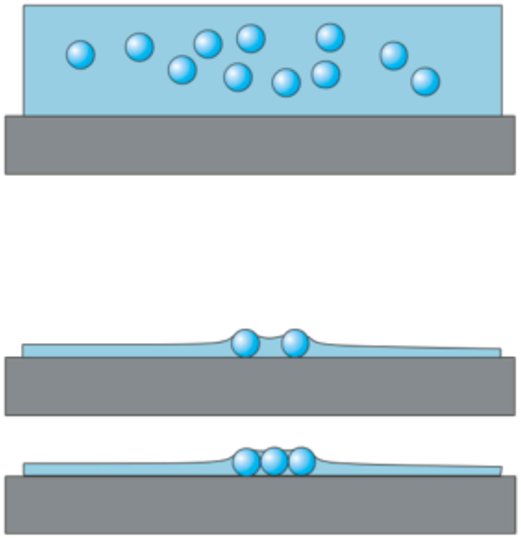

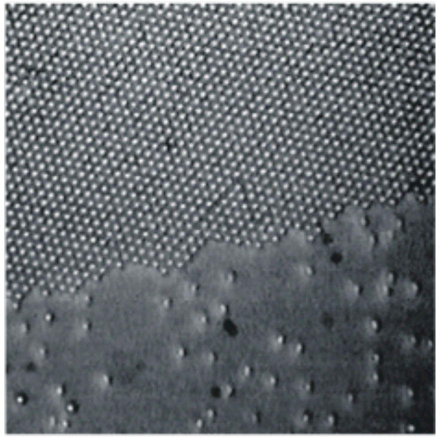

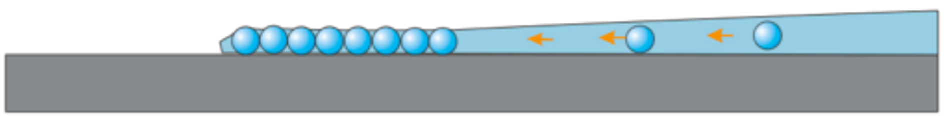

Two approaches:

- Spin coating
  [Hulteen, van Duyne J. Vac. Sci. Technol. A (1995)]
- Drying of the tilted substrate
  [Micheletto *et al*. Langmuir (1995)]

Liquid–air interface

1. Spreading of the particle suspension

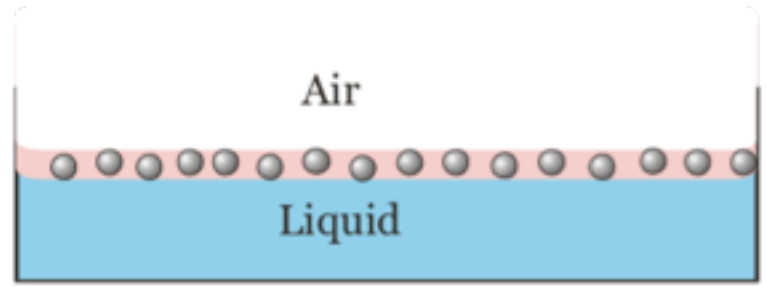

2. Application of a lateral pressure

→ Langmuir–Blodgett technique

→ Surfactant

3. Transfer to the solid substrate

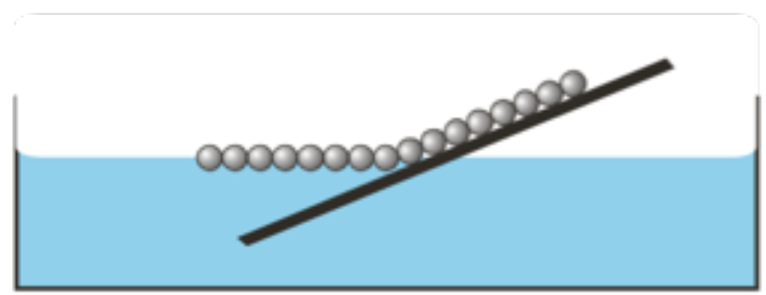

Self-assembled 2D arrays

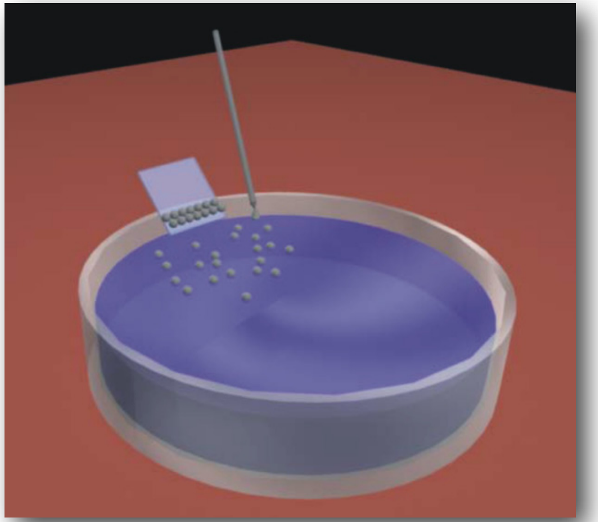

Pipette polystyrene spheres on a carrier

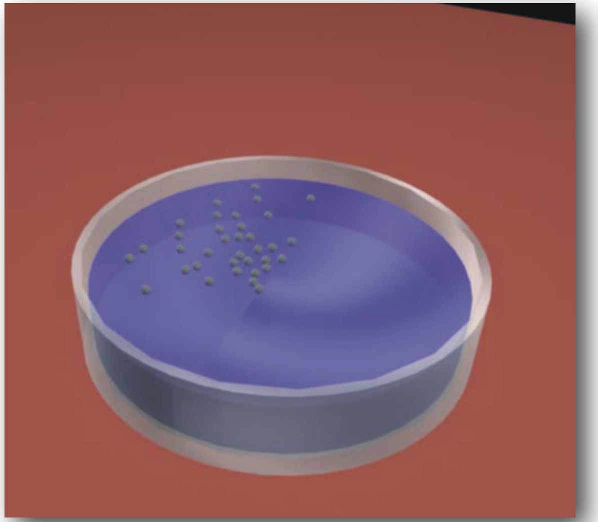

Spread of PS spheres on the water surface

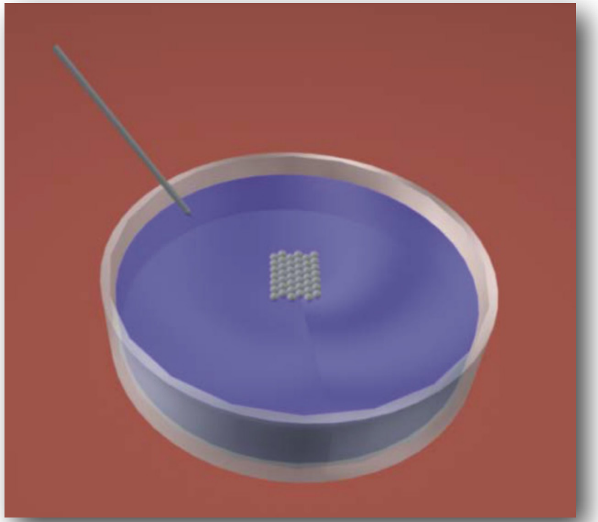

Transformation into a hexagonal array

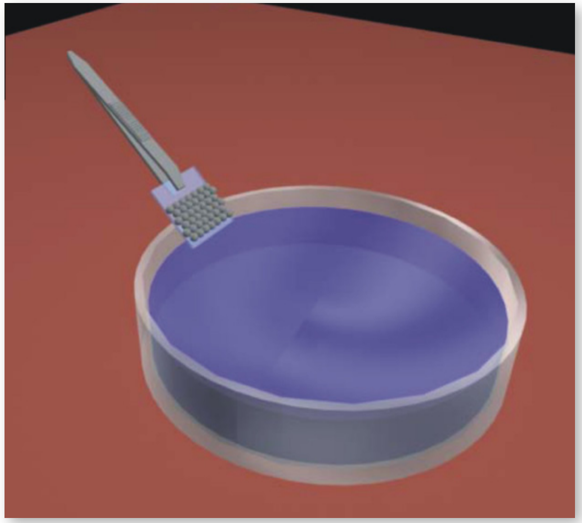

Mask transfer to the substrate

Modification of the apertures

- Thermal treatment of the mask slightly below the glass transition temperature: fusion of the spheres
- Control of the apertures by time and temperature

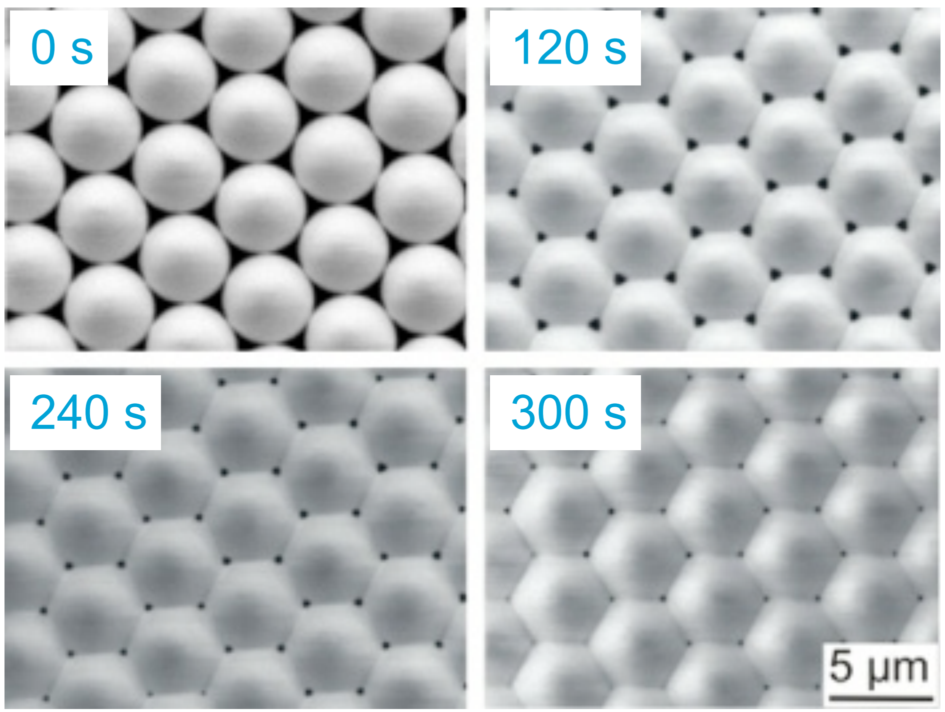

Thermal treatment at 118 °C

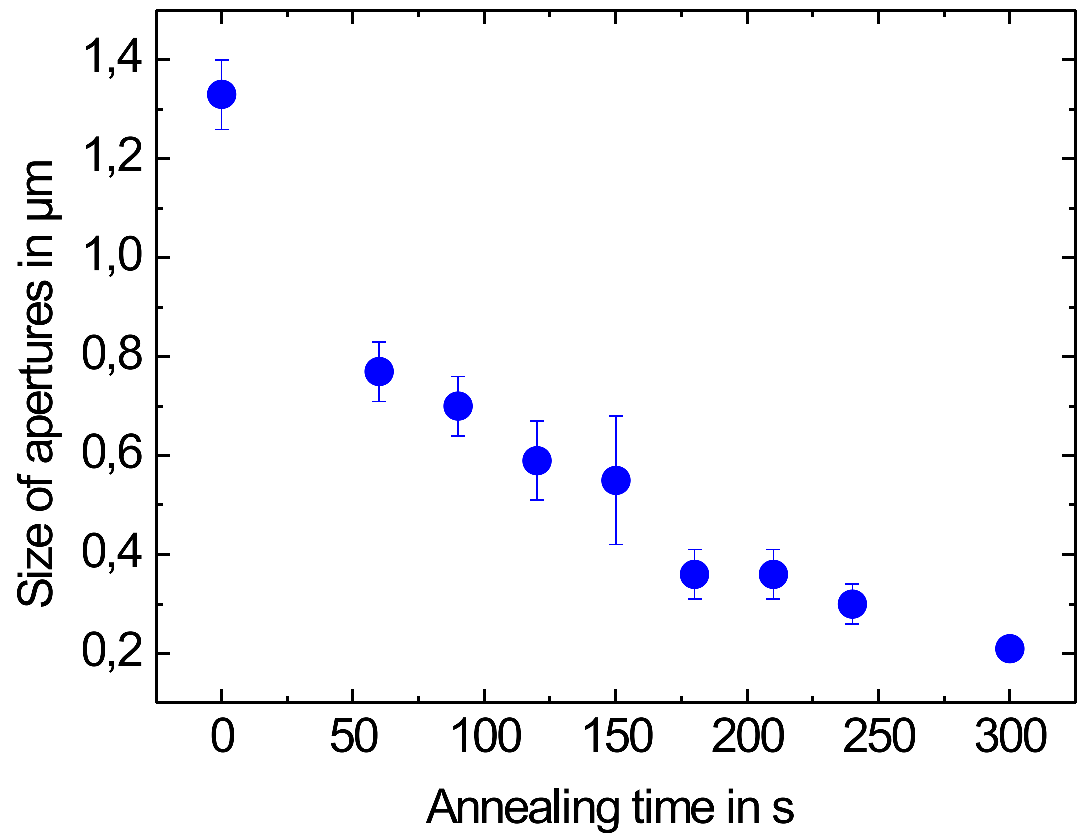

Fabrication of the evaporation source

- Tungsten wire bend into a particular shape
- Nickel deposition on the wire by electroplating
  (nickel sulfamate/boric acid electrolyte, 10 μm thick coating)

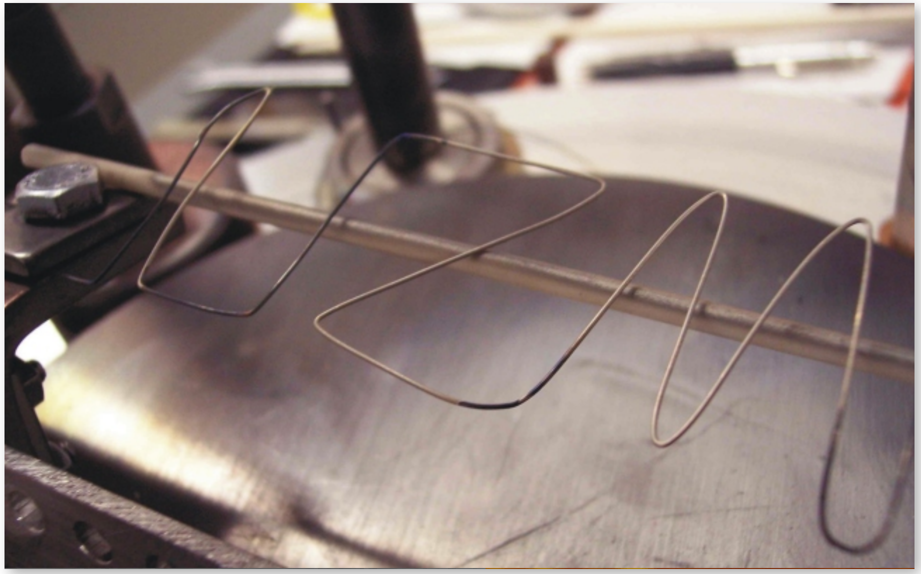

Shaped wire

Formation of shaped replicas

(a)

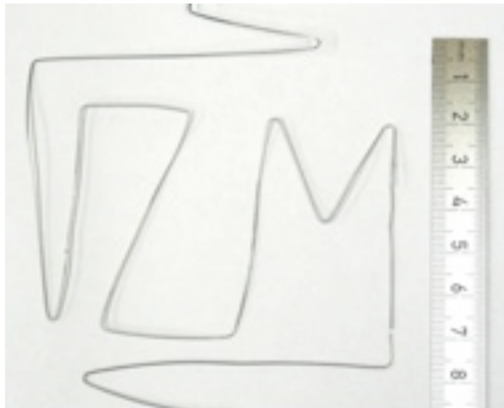

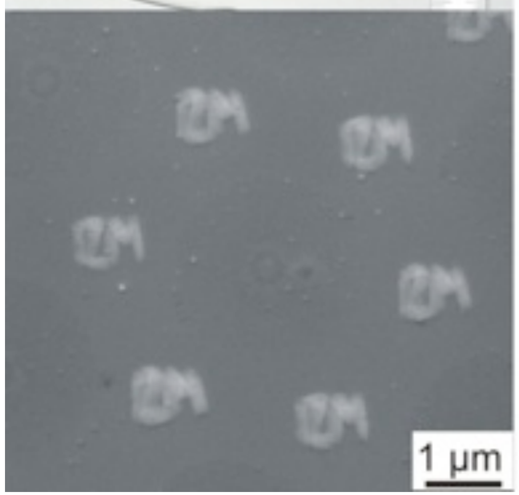

(b)

(c)

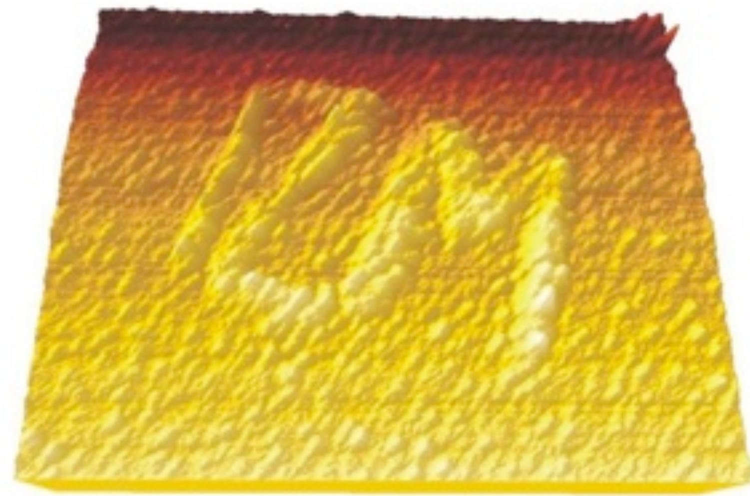

(*a*) Shaped wire used as the object with segments forming the letters I, Z, M covered by Ni

(*b*) Regular pattern of Ni replicas formed through the holes of the PS mask on the substrate

(*c*) Atomic force microscopy of a single picture (dimensions of the letter I: $700 \times 3 \times 130$ nm^3)

Imaging process

(a)

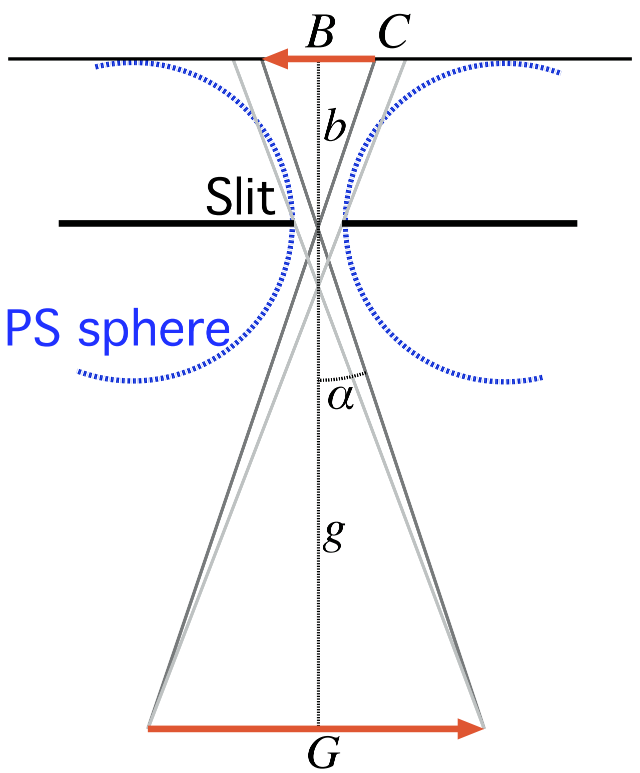

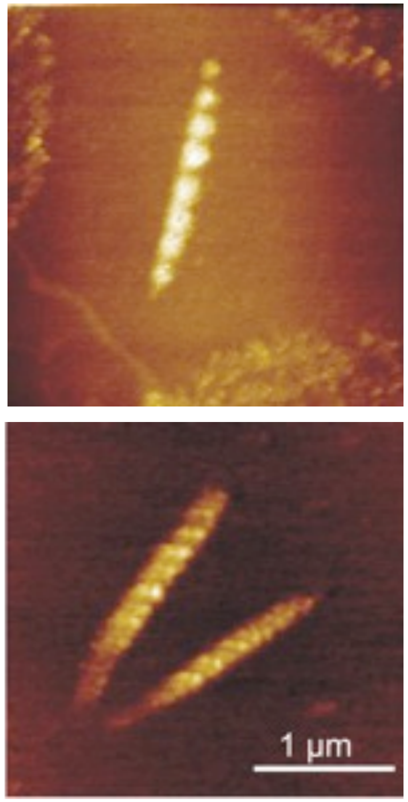

(c)

(b)

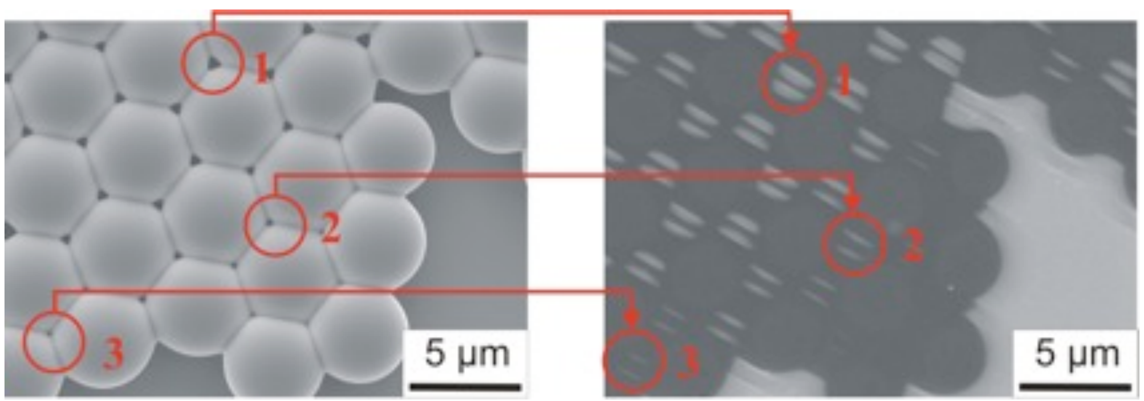

(*a*) Geometry of image formation

(*b*) Nanobars resulting from different aperture sizes

(*c*) Truncation of the replicas for smaller apertures

Finite width of the apertures

- The intercept theorem gives the image size:

$$B = \frac{Gb}{g}$$

  (G, g size, distance of the object)
- The image distance b corresponds to the radius of the PS spheres.
- Due to the finite width of the opening, the image is surrounded by a circle of confusion

$$C = \left(1 + \frac{b}{g}\right)\frac{P}{2}$$

- With $g \gg b$, the circle of confusion C is determined only by the aperture size P.

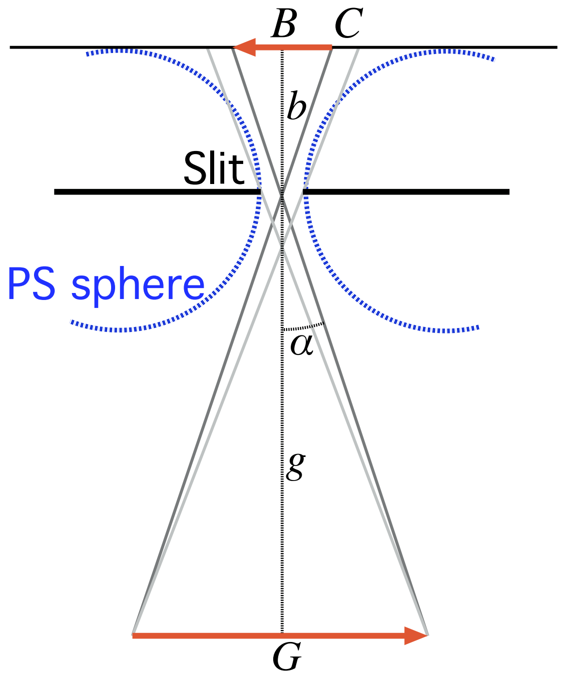

Effective viewing angle

- Maximum incident angle α for apertures formed by PS sphere masks: 48°
- The thermal treatment deforms the PS spheres and thus the planar apertures transform into cylindrical channels of the length h
- Reduced incident angle α' determined by

$$\tan\alpha' = \frac{P}{h}$$

- $\alpha' \approx \alpha/2$ from the experiment
- As a result of the reduction of the incident angle, a truncation of the replicas for apertures below 80 nm is observed due to the shadowing of the particle beam by the cylindrical opening.

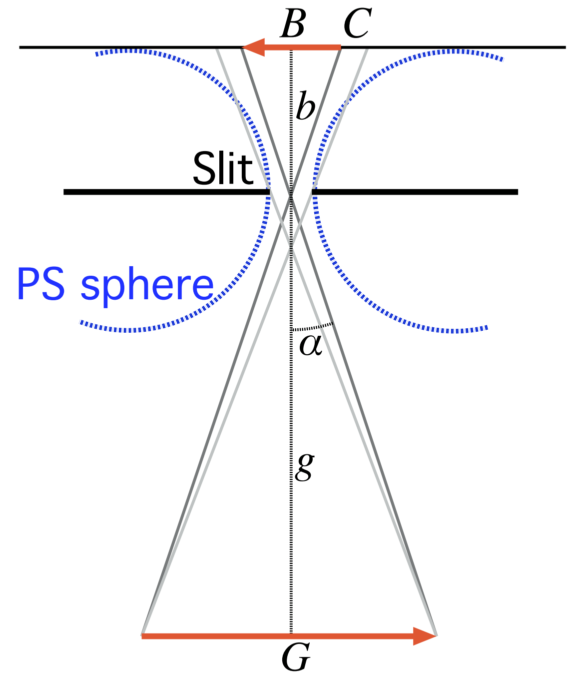

Intensity

- Finite size of the opening $\Rightarrow$ blurred image
- Infinitely small hole $\Rightarrow$ infinitely low intensity of the beam
- Effective intensity (proportional to the deposition rate) has been proven to depend linearly on the size of the hole,

$$I = P/b$$

- Demagnification B/G of 1:400 000 possible
- Aperture sizes of 50 nm have been achieved; line widths of the replicas as low as 30 nm feasible

Possibilities and limitations

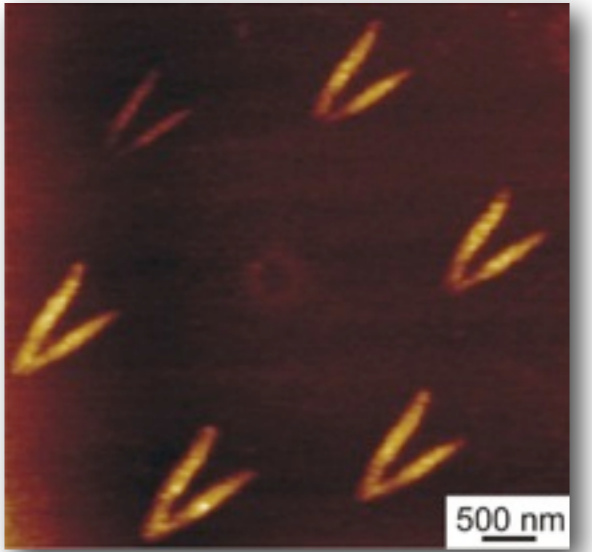

- In contrast to electron beam lithography or focused ion beam techniques, colloid lithography characterized by a parallel working principle
- Effective and low-cost technique with a high throughput for rather complex nanostructures
- No diffraction limit exist, no aberrations
- Optimization of the holes necessary by the improvement of the treatment of the mask in order to minimize the blurring
- Truncation problem can be solved by limiting the incident angle.

Summary

Colloid lithography can be used for the fabrication of various regular structures on the surface of wafers. Bottom up or top down approaches to produce nanostructures are possible for various applications, *e. g.* in the field of metamaterials, preparation of nanoantenas, nanowires, or for sensor applications. It is a relatively cheap method, which easily can be combined with various deposition techniques and plasma etching processes in a laboratory scale.

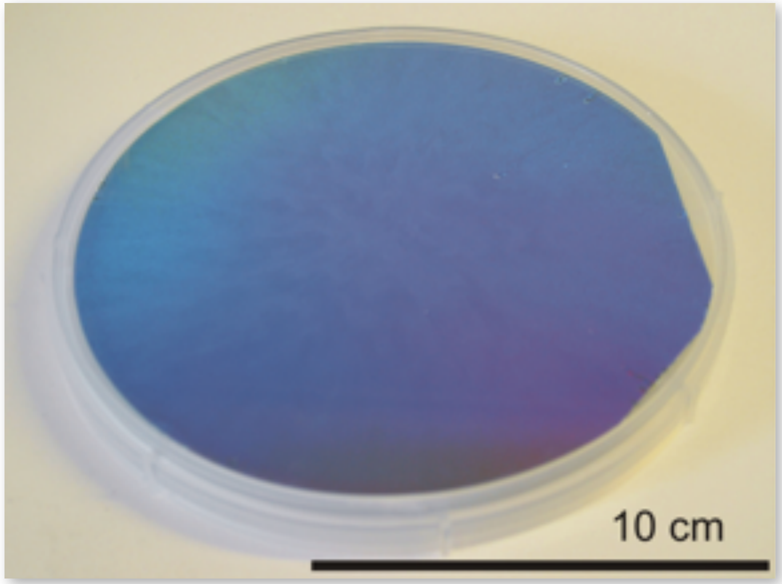

5″ Si (111) wafer with a mask of 508 nm polystyrene particles

Literature

- F. Burmeister *et al.*: Langmuir **13** (1997) 2983.
- J. C. Hulteen, R. P. Van Duyne: J. Vac. Sci. Technol. A **13** (1995) 1553.
- R. Micheletto *et al.*: Langmuir **11** (1995) 3333.